Report F49620-80-C-0023
Final Report
Project No. 2301/A1

G.L. Report No. 3520

RESEARCH STUDIES ON RADIATIVE COLLISIONAL PROCESSES

S. E. Harris
J. F. Young
Edward L. Ginzton Laboratory
W. W. Hansen Laboratories of Physics
Stanford University
Stanford, California 94305

November 1982

Final Report for Period 1 October 1979 – 30 September 1982

Contract Monitor:

Dr. Howard R. Schlossberg
AFOSR/NP
Bolling Air Force Base
Building 410
Washington, D.C. 20332

UNCLASSIFIED

SECURITY CLASSIFICATION OF THIS PAGE (When Data Entered)

REPORT DOCUMENTATION PAGE	READ INSTRUCTIONS BEFORE COMPLETING FORM
1. REPORT NUMBER: AFOSR-TR- 83 - 0428	2. GOVT ACCESSION NO.: AD-A128533
	3. RECIPIENT'S CATALOG NUMBER
4. TITLE (and Subtitle): RESEARCH STUDIES ON RADIATIVE COLLISIONAL PROCESSES	5. TYPE OF REPORT & PERIOD COVERED: Final Report 1 Oct. 79 – 30 Sept. 82
	6. PERFORMING ORG. REPORT NUMBER: G.L. Report No. 3520
7. AUTHOR(s): S. E. Harris, J. F. Young	8. CONTRACT OR GRANT NUMBER(s): F49620-80-C-0023
9. PERFORMING ORGANIZATION NAME AND ADDRESS: Edward L. Ginzton Laboratory, Stanford University, Stanford, California 94305	10. PROGRAM ELEMENT, PROJECT, TASK AREA & WORK UNIT NUMBERS: 61102F, 2301/A1
11. CONTROLLING OFFICE NAME AND ADDRESS: Air Force Office of Scientific Research, Bolling Air Force Base, Building 410, Washington, D.C. 20332	12. REPORT DATE: November 1982
	13. NUMBER OF PAGES: 45
14. MONITORING AGENCY NAME & ADDRESS (if different from Controlling Office)	15. SECURITY CLASS. (of this report): UNCLASSIFIED
	15a. DECLASSIFICATION/DOWNGRADING SCHEDULE

16. DISTRIBUTION STATEMENT (of this Report)

Approved for public release; distribution unlimited

17. DISTRIBUTION STATEMENT (of the abstract entered in Block 20, if different from Report)

18. SUPPLEMENTARY NOTES

19. KEY WORDS (Continue on reverse side if necessary and identify by block number)

Laser Induced Collisions
XUV Spectroscopy
Excimer Lasers

20. ABSTRACT (Continue on reverse side if necessary and identify by block number)

This program has supported theoretical and experimental studies in several areas of device physics: the physics and applications of radiative collisional lasers, pair absorption pumped lasers, the use of microwave pumping for the excitation of excimer and other high pressure lasers, and the development of anti-Stokes spectroscopy for the study of core-excited atomic levels.

DD FORM 1 JAN 73 1473 EDITION OF 1 NOV 65 IS OBSOLETE
S/N 0102-LF 014-6601

UNCLASSIFIED

SECURITY CLASSIFICATION OF THIS PAGE (When Data Entered)

I. INTRODUCTION

This program has supported theoretical and experimental studies in several areas of device physics: the physics and applications of radiative collisional lasers, pair absorption pumped lasers, the use of microwave pumping for the excitation of excimer and other high pressure lasers, and the development of anti-Stokes spectroscopy for the study of core-excited atomic levels. Section II lists some of the key results of this program; Section III summarizes our research findings; and Sections IV and V list the publications and the personnel, respectively, supported by this program.

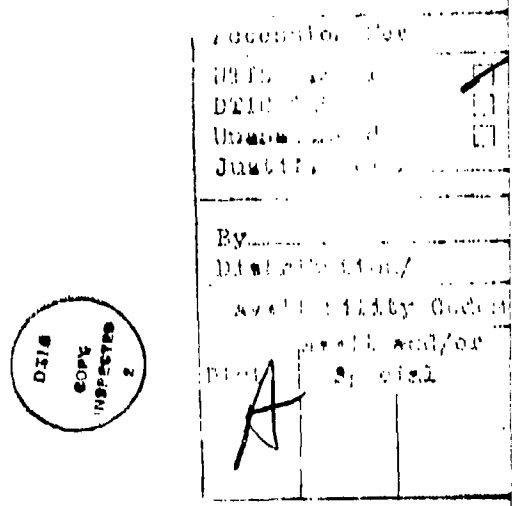

II. KEY RESULTS

Key accomplishments of our research group that bear on this program are as follows:

(1) Laser induced collisions were demonstrated for the first time in our group at Stanford in 1976.[1]

(2) Collision cross sections approaching 10^{-12} cm^2, at large laser power density were shown by Green, et al.[2]

(3) Laser induced dipole-quadrapole[3] and laser induced charge transfer processes were demonstrated[4] and studied.[5]

(4) The process of radiative collisional fluorescence was observed by White, et al.[6] The key prediction of a relatively narrow emission width, centered at the $R = \infty$ wavelength of the separated atoms was confirmed.

(5) Pair absorption in atomic systems was demonstrated for the first time.[7]

(6) The first pair absorption pumped laser was constructed by Falcone and Zdasiuk.[8]

(7) Microwave pumping of a high pressure XeCl excimer laser was demonstrated.[9]

(8) The anti-Stokes radiation source was used for core-excited absorption spectroscopy of K. A resolution at 500 Å of about 1.3 cm^{-1} was obtained.[10]

(9) A pulsed, all metal, hollow cathode discharge was developed under ONR support by Falcone, et al.[11] Population densities in the resonance line of Li of 4×10^{16} atoms/cm^3 were obtained

under conditions where populations of higher levels were very much smaller (about 10^{13} atoms/cm^3).

(10) Harris, et al.[12] have noted near energy coincidences in the alkali atoms which may allow the construction of radiative collisional lasers.

References

1. S. E. Harris, R. W. Falcone, W. R. Green, D. B. Lidow, J. C. White, and J. F. Young, "Laser Induced Collisions," in Tunable Lasers and Applications, A. Mooradian, T. Jaeger, and P. Stokseth, eds. (New York: Springer-Verlag, 1976); R. W. Falcone, W. R. Green, J. C. White, J. F. Young, and S. E. Harris, "Observation of Laser Induced Inelastic Collisions," Phys. Rev. A 15, 1333 (March 1977); and S. E. Harris, J. F. Young, R. W. Falcone, W. R. Green, D. B. Lidow, J. Lukasik, J. C. White, M. D. Wright, and G. A. Zdasiuk, "Laser Induced Collisional Energy Transfer," in Atomic Physics VII, D. Klepner and F. M. Pipkin, eds. (New York: Plenum Press, 1981).

2. W. R. Green, J. Lukasik, J. R. Willison, M. D. Wright, J. F. Young, and S. E. Harris, "Measurement of Large Cross Sections for Laser-Induced Collisions," Phys. Rev. Lett. 42, 970 (April 1979).

3. W. R. Green, M. D. Wright, J. Lukasik, J. F. Young, and S. E. Harris, "Observation of a Laser Induced Dipole-Quadrupole Collision," Optics Lett. 4, 265 (September 1979).

4. W. R. Green, M. D. Wright, J. F. Young, and S. E. Harris, "Laser Induced Charge Transfer to an Excited Ionic State," Phys. Rev. Lett. 43, 120 (July 1979).

5. M. D. Wright, D. M. O'Brien, J. F. Young, and S. E. Harris, "Laser Induced Charge Transfer Collisions of Calcium Ions With Strontium Atoms," Phys. Rev. A 24, 1750 (October 1981).

6. J. C. White, G. A. Zdasiuk, J. F. Young, and S. E. Harris, "Observation of Radiative Collisional Fluorescence," Phys. Rev. Lett. 41, 1709 (December 1978).

7. J. C. White, G. A. Zdasiuk, J. F. Young, and S. E. Harris, "Observation of Atomic Pair Absorption With an Incoherent Source," Optics Lett. 4, 137 (May 1979).

8. R. W. Falcone and G. A. Zdasiuk, "Pair Absorption Pumped Barium Laser," Optics Lett. 5, 155 (April 1980).

9. A. J. Mendelsohn, R. Normandin, S. E. Harris, and J. F. Young, "A Microwave Pumped XeCl* Laser," Appl. Phys. Lett. 38, 603 (April 1981); and J. F. Young, S. E. Harris, P. J. K. Wisoff, and A. J. Mendelsohn, "Microwave Excitation of Excimer Lasers," Laser Focus (April 1982), p. 63.

10. Joshua E. Rothenberg, J. F. Young, and S. E. Harris, "High Resolution XUV Spectroscopy of Potassium Using Anti-Stokes Radiation," Optics Lett. 6, 363 (August 1981); and S. E. Harris, J. F. Young, R. W. Falcone, Joshua E. Rothenberg, J. R. Willison, and J. C. Wang, "Anti-Stokes Scattering as an XUV Radiation Source and Flashlamp," in Laser Techniques for Extreme Ultraviolet Spectroscopy, R. R. Freeman and T. J. McIlrath, eds. (New York: AIP, 1982) (to be published).

11. R. W. Falcone and K. D. Pedrotti, "Pulsed Hollow Cathode Discharge for XUV Lasers and Radiation Sources," Optics Lett. 7, 74 (February 1982); and R. W. Falcone, D. E. Holmgren, and K. D. Pedrotti, "Hollow-Cathode Discharge for XUV Lasers and Radiation Sources," in Laser Techniques for Extreme Ultraviolet Spectroscopy, R. R. Freeman and T. J. McIlrath, eds. (New York: AIP, 1982) (to be published).

12. S. E. Harris, R. W. Falcone, and D. M. O'Brien, "Proposal for High Power Radiative Collisional Lasers," Optics Lett. 7, 397 (September 1982).

III. SUMMARY OF RESEARCH

A. RADIATIVE COLLISION AND PAIR ABSORPTION LASERS

For several years we have been developing technology for the electrical excitation of relatively high density (10^{17} atoms/cm^3) alkali atoms. In a high density discharge the near unity oscillator strength of the resonance transition accomplishes several functions. First, an average electron makes an inelastic collision with a resonance line atom about once every 10 ps and, therefore, until the resonance line is sufficiently populated to allow super-elastic collisions, the temperature of the electrons is closely pinned to the resonance line energy. Second, the large oscillator strength results in radiative trapping times of at least several μs, so that spontaneous radiative decay is not of consequence.

During the contract period we suggested the use of the radiative-collisional laser process for the extraction of energy which is stored in the resonance lines of the alkali atoms. The suggestion was motivated in part by a recent experiment with a pulsed hollow-cathode discharge where Falcone and co-workers have obtained a population in the upper level of the resonance line of lithium of 4×10^{16} atoms/cm^3, corresponding to a stored energy density of about 0.01 J/cm^3. This population is stable for a 75 ns period, and occurs under conditions where the population of higher levels, for example the Li ($1s^2 3p$) and Li ($1s^2 3d$) levels, are much lower (about 10^{13} atoms/cm^3).

A prototype of the alkali atom systems which we considered is shown in Fig. 1. Initially, two atoms are excited by a discharge to the $3p\ ^2P_{1/2}$ level of the sodium resonance line transition. During the collision between

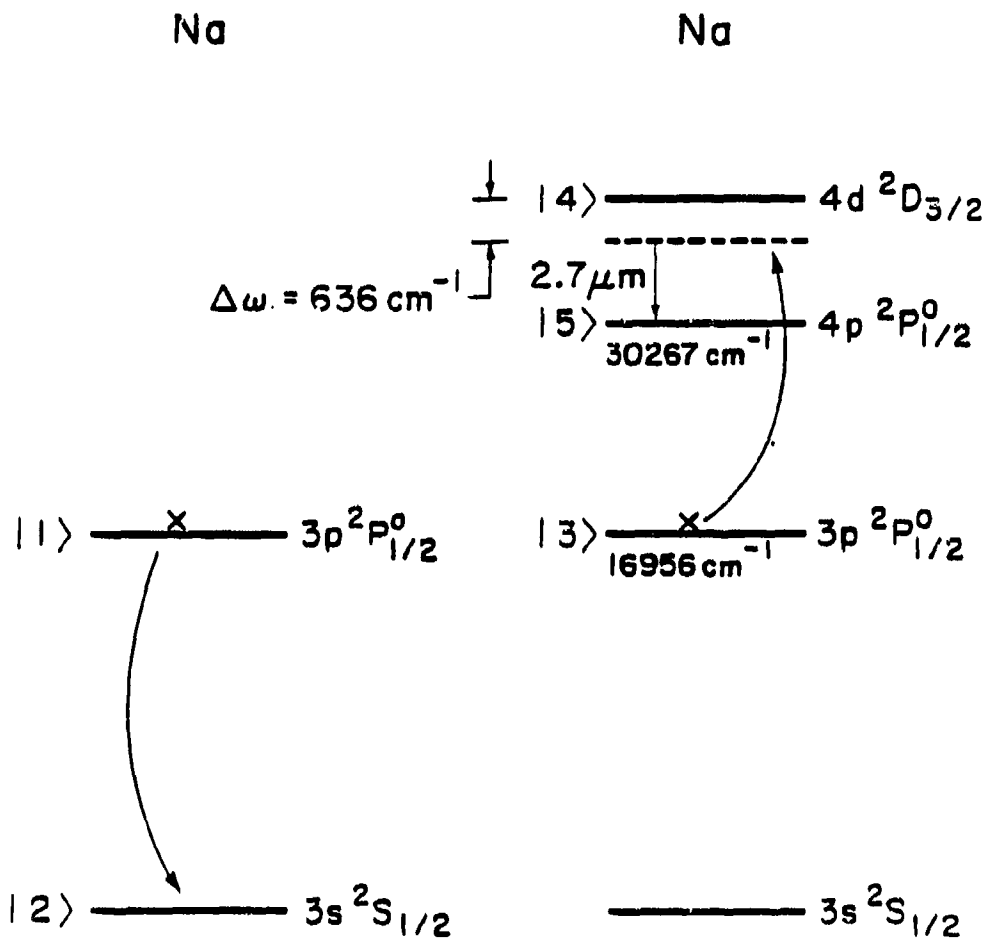

Fig. 1--Prototype system for alkali atom radiative collision laser.

the excited atoms dipole-dipole coupling causes a simultaneous transition of one atom to the ground level and the other atom to a virtual level (shown by the dotted line) which has 4d character. The radiative-collisional process is completed by the emission of a photon at 2.7 μm, thereby resulting in the de-excitation of both resonance line atoms.

The photon at 2.7 μm may be emitted spontaneously, or of interest to us here, may be stimulated. The lineshape for both spontaneous emission and gain will center at a frequency equal to twice that of the resonance line minus that of the terminal level; and for the system considered here will have a width of 10 to 20 cm^{-1}. The requirement for net radiative collisional gain is that the product of the densities of the excited resonance atoms exceed the product of the ground and final level ($1s^2 4p\ ^2P^o_{1/2}$) densities.

Table 1 gives the results of our calculations for a number of alkali systems. We limit the table to systems where only a single element is used, and where storage is in the resonance level of the atom. The particular fine structure component of the np^2P level in each of the atoms is denoted in column 1. The calculated gain (per cm) assumes a storage density of 5×10^{16} atoms/cm^3 in each of the storage levels; and varies as the square of this number. The parameter ρ_0 in the third column gives a guide to the maximum rate of energy extraction from the system. At large power densities (for these systems, typically 10^9 W/cm^2) the cross section for laser induced collision is several times $\pi\rho_0^2$. At a gas density of 5×10^{16} atoms/cm^3, this corresponds to a collision frequency of about 10^9 and therefore a maximum energy extraction rate of about a nanosecond.

Table 1

Alkali Atom Radiative Collision Lasers

Element and Storage Level[a]	$\lambda(\mu m)$	$\rho_0(\mathring{A})$	$g(cm^{-1})$ [b]
Na (1/2 , 1/2)	2.7	15.0	1.4×10^{-3}
Rb (3/2 , 3/2)	5.4	15.7	8.0×10^{-2}
Rb (1/2 , 3/2)	6.3	16.0	3.4×10^{-3}
Cs (3/2 , 3/2)	6.6	20.6	3.6×10^{-3}
Cs (1/2 , 3/2)	10.3	27.9	1.1×10^{-2}

[a] In all cases the storage levels are the ^2P_J levels of the resonance line, where J is indicated in column 1.

[b] The gain (per cm) is calculated with an assumed storage density of 5×10^{16} atoms/cm^3.

The highest gain system is one in which two excited state rubidium atoms (5p) collide to produce a ground state Rb atom, an excited state Rb atom (6p) and a photon at 5.4 μm. At a resonance line population of 5×10^{16} atoms/cm^3 the calculated gain is 8% per cm.

A suitable discharge has been constructed which is capable of producing ~ 10^{16} atoms/cm^3 in the storage state. A tunable infrared source (difference mixing in $LiIO_3$) and cooled detectors (HgCdTe) coupled with a computer and data display system allow sensitive gain measurements to be performed despite the electrically noisy environment produced by the hollow-cathode discharge. Current sensitivity is 8%. With our measured population, cell length and double pass configuration the gain at 5.4 μm should be ~ 6%. Experimental runs to date have shown no evidence of gain. This is understandable given the uncertainty in our measurement of storage state population.

Most recently our efforts have been concentrated on maximizing the resonance line population levels by optimizing the cathode design. The figure of merit for a cathode can be defined as the product of the square of the resonance line population and the zone length over which this population exists – $N(5p)^2 \times \ell$. This factor multiplied by the radiative collisional gain factor g yields the per pass gain coefficient. Our best cathode produces $N^2\ell = 2.8 \times 10^{32}$. For the Rb system, $g = 1.9 \times 10^{-35}$ which implies a 0.06% gain per pass. Clearly, more work has to be done on improving the population of the Rb resonance line. However, with the existing apparatus it is possible to perform an experiment which would verify the shape and position of the expected gain as well as provide an indication of the magnitude of the effect.

This experiment is essentially a laser-induced collision laser. The scheme is the same as for the radiative-collision laser with the exception that the goal is to transfer a large population to the $6p_{3/2}$ state via the radiative-collisional transition at 5.4 μm. The $6p_{3/2}$ state will then be inverted with respect to the $6s_{1/2}$ (2.7 μm). The population of the $6p_{3/2}$ can be calculated as

$$N(6p_{3/2}) = \frac{P/A}{\hbar\omega} \alpha\tau$$

where $\alpha = gN^2$, τ is the length of the pump pulse, and $\frac{P/A}{\hbar\omega}$ is the number of photons/cm^2 in the pump pulse at 5.4 μm. With 1 kW of infrared $N(6p_{3/2}) = 3 \times 10^{13}$ cm^{-3}, which implies a gain of e^{143} in 1.7 cm. However, we must first measure the $6s_{1/2}$ population in order to verify that its population is small compared with 10^{13} cm^{-3}.

The observation of lasing at 2.7 μm will be interesting in its own right as it will be the first demonstration of a radiative collision pumped laser utilizing discharge methods to create the initial (storage) state.

B. MICROWAVE EXCITATION OF HIGH PRESSURE GAS SYSTEMS

1. Introduction

Simple, efficient methods of exciting high pressure (1 atmosphere and above) gas mixtures are of considerable practical interest. This interest stems from the development of several useful, or potentially useful, lasers which require such pressures, including the rare gas halide (RGH) dimer excimer lasers, RGH trimer excimers, and rare gas excimers. In addition, there is interest in high pressure operation of CO_2 lasers

to achieve continuous tuning via pressure broadening; our proposals for new radiative collisional lasers also rely on the excitation of high pressure gas systems.

Over the past six years RGH dimer lasers (XeF, XeCl, ArF, etc.) have progressed from being a scientific curiosity to viable commercial products which are experiencing increasing applications because of their ability to provide high powers in the difficult-to-access UV spectral region. The rare gas excimers Xe_2 and Ar_2 can provide tunable radiation at 173 nm and 126 nm, respectively. Although such sources have many exciting potential applications to spectroscopy, photochemistry, surface studies, and lithography, little work has been done because of the complications of electron beam excitation. The recently studied RGH trimer lasers such as Xe_2Cl offer wide tunability in the visible region: Xe_2Cl at 490 ± 40 nm, Xe_2F at 630 ± 50 nm, and Kr_2F at 420 ± 35 nm have been observed to date using electron beam excitation.

Up until the past year only two methods had been used to excite excimer lasers: direct electron beam ionization, and the use of pulsed electrical discharges. Under this program we have been studying a third technique, the use of high power microwave pulses. To date most of our work has used XeCl, one of the higher gain, least corrosive RGH combinations. Our results have been encouraging and indicate that this approach may have practical application for the systems mentioned. In particular, we have succeeded in producing long-pulsed (200 ns) XeCl excimer lasers in a relatively simple apparatus. In addition, spontaneous fluorescence pulse lengths of over 500 ns verify the ability of microwaves to effectively excite such systems for long times without instabilities. In addition, we have studied the

coupling of microwave power into pure rare gases up to pressures of 17 atmospheres and have observed high coupling efficiencies.

2. Comparison of Conventional and Microwave Excitation

Electron beam pumped RGH lasers have exhibited the highest efficiencies (5% for $XeCl^*$), but their large size, high cost, low repetition rates, and complexity have generally restricted them to large scale, dedicated applications. Most laboratory and all commercial RGH dimer excimer lasers are excited using a transverse, self-sustained avalanche discharge because of its relative simplicity and good performance. Although efficiencies of 1% have been achieved, the characteristics of such excitation are extremely dependent on the discharge conditions; the pulse length and efficiency are limited by the formation of plasma arcs which make it impossible to maintain adequate excitation rates throughout the gas volume for times in excess of ~ 20 ns. The problem becomes even more severe at pressures above ~ 4 atm. Thus laser action in the RGH trimers, which require pressures of > 6 atm., and in the rare gas excimers, which require 15-20 atm. pressures, has been achieved only using electron beam excitation. In contrast, microwave pumping exhibits much less sensitivity to gas conditions than the avalanche discharge while retaining much of its practical simplicity.

The sensitivity of avalanche discharges to such factors as detailed gas composition, electrode irregularities, degree and uniformity of preionization, and the characteristics of the driving source have been described in detail by Levatter and Lin. They note that because of these problems avalanche discharge laser pulse lengths have been limited to about 10 ns, except for their own work using x-ray preionization and very fast rise time drivers, and for the work of Hogan, Kearsley, and Webb

using a system of resistively stabilized pin electrodes. Pulse lengths of ~ 10 ns are too short to permit the development of good spatial modes, narrow bandwidths, or short mode-locked pulses.

In contrast, microwave excitation of high pressure gases is much less sensitive to the details of the plasma: the power deposition is nominally independent of gas composition, uniform preionization is not critical, and even a local breakdown or arc as not prevent excitation in other regions of the plasma. The basic configuration for microwave heating is shown in Fig. 2. A dielectric tube, such as quartz, confines the laser mixture to a small region of a waveguide carrying the microwave power. The electric field of the microwaves can penetrate the gas and heat the electrons as long as the relative dielectric permittivity ϵ of the plasma remains near 1. At large values of n_e, $|\epsilon|$ becomes large, and the internal field and electron heating are significantly reduced. This shielding or impedance mismatch takes place when the plasma frequency equals the incident microwave frequency, ω, or the electron collision frequency, ν_c, whichever is higher. At pressures above ~ 500 torr the latter generally dominates for incident frequencies of several GHz. For He at 2 atm., $\nu_c = 3 \times 10^{12}$ and the limiting n_e is about 10^{15} cm^{-3}. Note that although a local increase in charge density can result in a decoupling of the field from the plasma, this shielding is purely local: the microwave field is not "shorted out" and continues to effectively excite the rest of the plasma volume. Of course, the creation of even a local large impedance mismatch in a poorly chosen geometry could result in large reflections of power and poor excitation efficiency.

For values of n_e below the critical value the gas column can be viewed as a lossy rod which absorbs power and attenuates the microwaves.

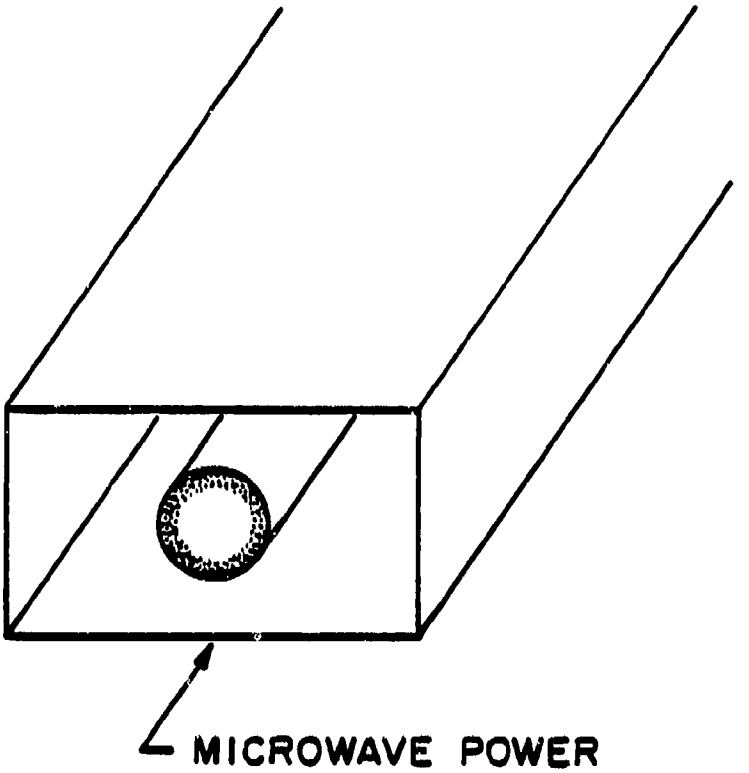

Fig. 2--Basic configuration for microwave excitation of a laser plasma.

In the idealized uniform plasma case the absorption can be characterized by a transverse skin depth δ_T . For $\nu_c \gg \omega$, and small n_e such that $\omega_p < \nu_c$

$$\delta_T \simeq \frac{mc\epsilon_0}{e^2} \frac{\nu_c}{n_e}$$

while near the limiting value of n_e such that $\omega_p \sim \nu_c$

$$\delta_T \simeq \sqrt{\frac{mc^2\epsilon_0}{2e^2} \frac{\nu_c}{\omega n_e}}$$

The change from a linear to square-root dependence on the quantity ν_c/n_e occurs at $\omega_p^2 \sim \omega\nu_c$ or $n_e \simeq 2 \times 10^{13}$ cm^{-3} for He at 2 atm. For uniform excitation δ_T should be at least equal to the tube radius r . This requirement is satisfied for typical conditions until n_e approaches the critical value, as illustrated in Table 2. Nevertheless, the results do indicate that microwave excitation is limited to relatively small bore, small volume systems.

For dense plasmas the power dissipation density is

$$P_D = \tfrac{1}{2} \epsilon_0 \omega |\epsilon|^2$$

where ϵ is the electric field in the waveguide. Thus P_D is independent of the detailed plasma conditions. Not explicitly shown, however, is the fact that the effective volume which is absorbing power is decreasing as n_e increases.

From the skin depth and a calculation of the microwave power dissipation per unit volume in the plasma one can compute the longitudinal

Table 2

Plasma Power Absorption Length and Relative Impedance as a Function of Electron Density

(1500 torr He, 9.4 GHz, 10 eV electron energy)

n_e	δ_T	$\lvert\eta/\eta_0\rvert$
1×10^{12} cm^{-3}	300 mm	1.0
3×10^{12} cm^{-3}	95 mm	1.0
1×10^{13} cm^{-3}	30 mm	0.99
3×10^{13} cm^{-3}	9.8 mm	0.94
1×10^{14} cm^{-3}	3.6 mm	0.72
3×10^{14} cm^{-3}	1.6 mm	0.43
1×10^{15} cm^{-3}	0.7 mm	0.24

attenuation of the microwave field as it propagates down the guide. This absorption length, δ_L , depends on both the plasma conditions and the fractional area of the guide filled with plasma. For a 4 mm diameter tube in an X-band WR-90 guide (23 mm × 10 mm) and $\delta_T = r$, $\delta_L = 18$ cm . Thus, in practice, the configuration of Fig. 2 would result in a short, nonuniform excitation region, and we developed a distributed coupling geometry to provide a longer, more uniform excitation length.

3. Experimental Results

Figure 3 illustrates the basic experimental configuration used in our experiments to date. A Varian SFD-303 coaxial magnetron and line-type pulser (a surplus airborne radar transmitter) provides 2 μs long pulses at 9.375 GHz. The microwave energy is coupled from the primary waveguide into a secondary guide containing a concentric quartz tube holding the gas mixture. Typically, tubes having a 3mm i.d. and an active length of 40 cm are used. The waveguides are pressurized with SF_6 to prevent breakdown at high microwave powers. The microwave coupler consists of a series of "Riblet Tee" slots in the common braod wall of the two guides. The size and spacing of the slots were adjusted to provide nearly uniform transfer of energy along the length. Using such techniques 80-90% of the input microwave energy could be absorbed in the gas mixture over a wide range of mixtures and pressures. For low power microwave inputs the discharge is more stable and reproducible if it is initiated by a small amount of preionization. This was accomplished by placing a ~ 12 cm long sealed quartz tube containing ~ 1 torr of Xe in the secondary guide. This low pressure "flashlamp" breaks down early in the microwave pulse providing simple, self-timed UV preionization of the laser mixture. At input powers above 0.7 MW the preionization is not necessary.

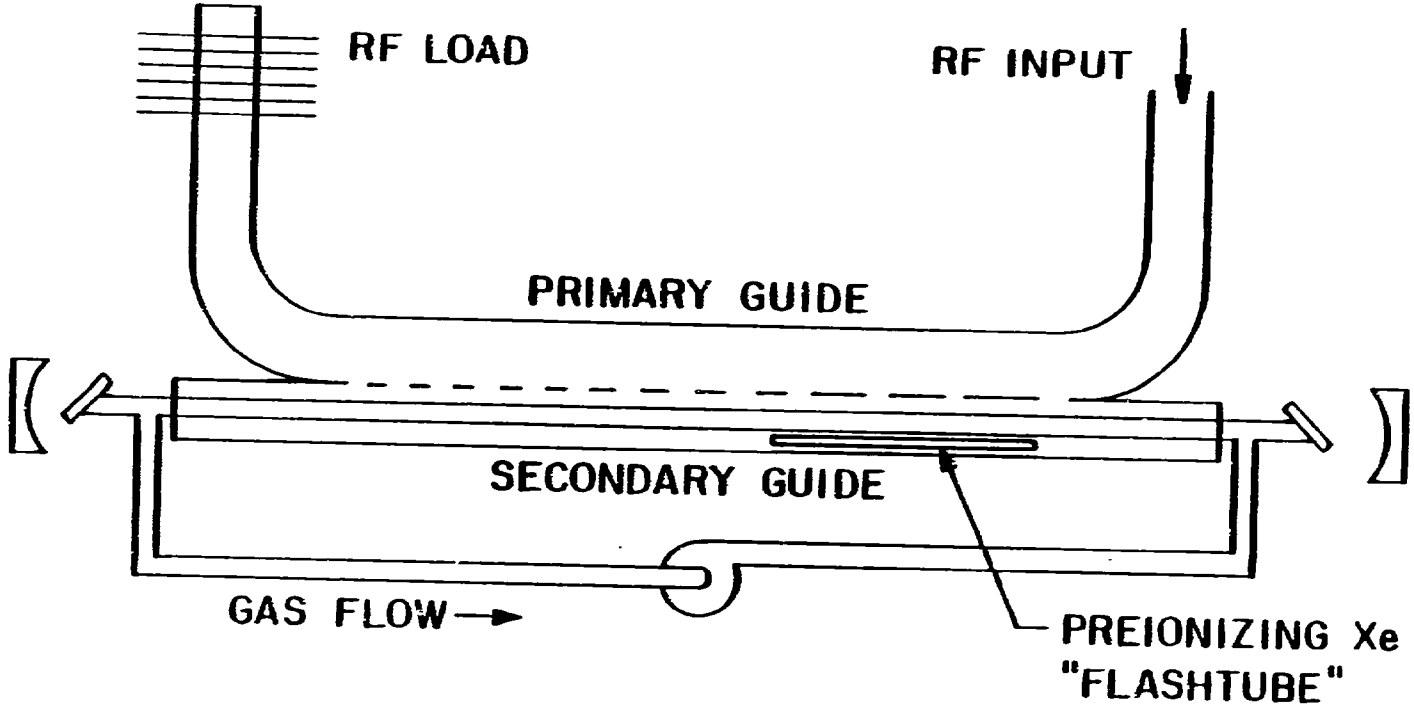

Fig. 3--Schematic of a microwave-pumped $XeCl^*$ laser. The Brewster windows are CaF_2 and the cavity consists of 2-m-radius mirrors 1 m apart.

In either case, once the discharge is initiated the power reflected to the source is insignificant. An all-stainless-steel closed loop system is used to circulate the gas mixture through the plasma tube.

In our first series of experiments the available microwave power was limited to about 600 kW and the secondary guide consisted of a standard WR-90 waveguide containing a 3 mm i.d. quartz tube. Laser action in $XeCl^*$ was observed at several wavelengths centered at 308 nm. Figure 4 shows the relative time behavior of the microwave, spontaneous fluorescence, and laser pulses for our optimum mixture of 0.3% Xe, 0.05% HCl, and 99.6% Ne at a total pressure of 2 atm. The long spontaneous emission time, over 500 ns FWHM, confirms the ability of microwaves to provide stable, long-term excitation of high pressure RGH mixtures. While the observed laser pulse length of 150 ns is 10 times longer than those of discharge systems, it is surprisingly short relative to the fluorescence pulse length. We have not yet determined the cause of this behavior; some possible mechanisms include build-up of a transient loss, kinetic bottlenecks, inhomogeneous excitation, and thermal or acoustic distortions of the optical path.

The maximum roundtrip gain in this system was about 20%. Using 5% output coupling the peak laser output was about 500 W, representing an efficiency of 0.1%. The normal repetition rate was 10 Hz, but rates up to 400 Hz were possible with significantly reduced performance because of our low longitudinal flow rates. It is interesting to note that our optimum gas mixture differs significantly from those normally used for avalanche discharge lasers, while it corresponds closely to one which minimizes transient losses at the laser wavelength. The insensitivity of the microwave excitation to details of the gas composition has permitted us

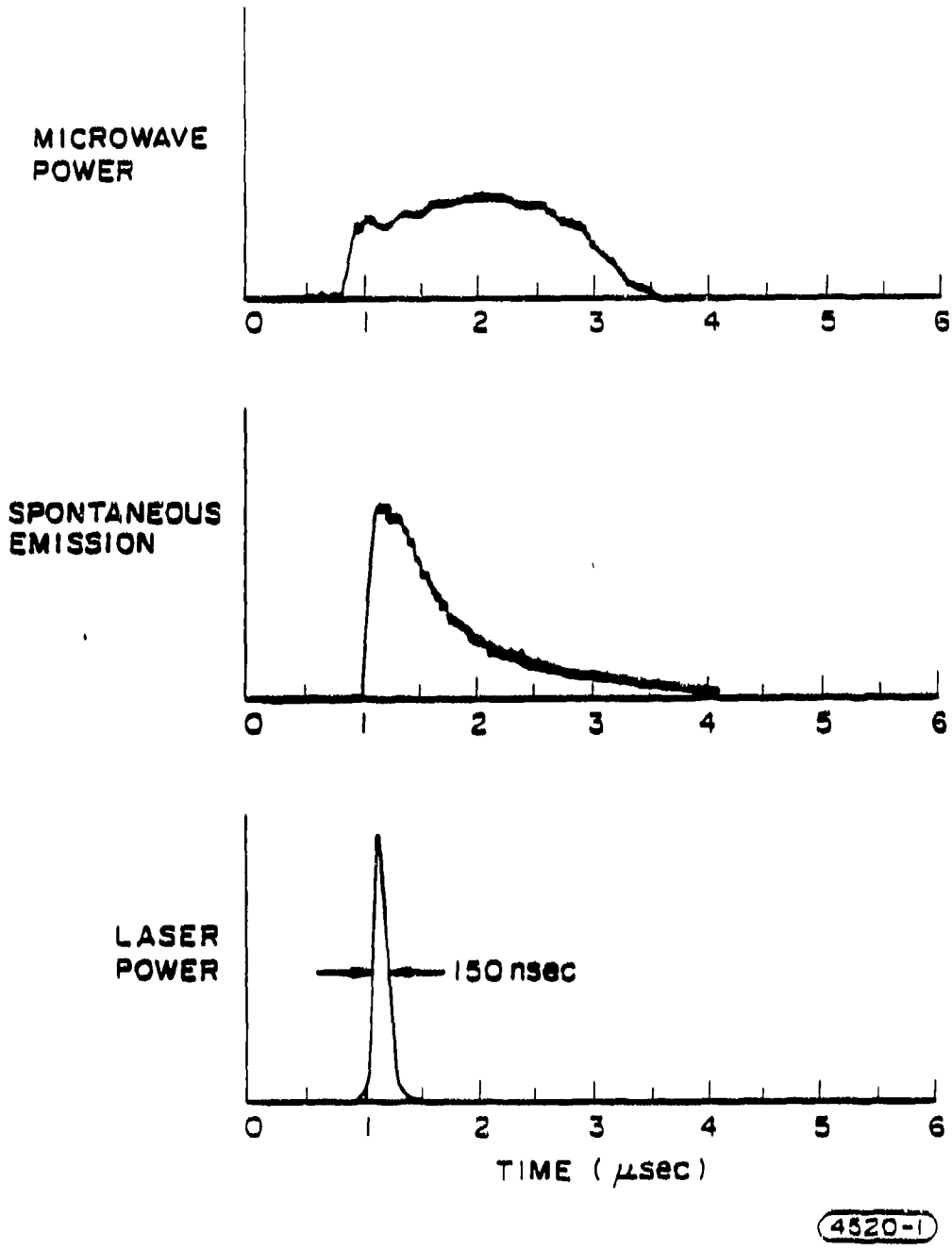

Fig. 4--Relative time behavior of the microwave power, $XeCl^*$ spontaneous emission, and laser pulses.

to choose gas mixtures on the basis of basic laser performance rather than for discharge behavior. No corrosion or breakage of the quartz plasma tube was observed; all lifetime problems originated in the flow system.

Presently we are using a new SFD-303B magnetron which can provide up to 1.4 MW, 3.5 μs long pulses. In addition, a new cell was designed in which the secondary guide area was reduced by decreasing the waveguide height to about 5 mm, the plasma tube outside diameter. An exchangeable coupling plate was used to permit optimization of microwave power deposition into the gain medium. Best results were obtained with a Riblet-Tee structure over the input half of the discharge length, followed by a completely open region between the two guides. No preionization was used. Figure 5 shows the behavior of this system. Following the initial breakdown, the microwave absorption was 100% for the first 500 ns of the pump pulse, and then decreased to 50% for the remainder of the pulse. Laser action occurred at the time of maximum fluorescence which coincided with the drop in microwave absorption. Compared to our earlier cell, we observed somewhat longer pulses, ~ 200 ns FWHM, but reduced peak powers, ~ 250 W. The net gains were higher than before, ~ 40% per roundtrip, so that larger output coupling may give improved powers and efficiency. At this higher excitation density our maximum pulse rate was limited to 190 Hz.

The microwave absorption in this cell was studied up to total pressures of 5 atm. Although the temporal behavior of the absorption was approximately constant, the effects of finite skin depth became evident as a ring of bright fluorescence at the circumference of the plasma tube. Our qualitative observations indicate that as the pressure is increased the peak n_e increases faster than ν_c, resulting in shorter skin depths and nonuniform excitation. Even at our optimum total pressure of 2 atm., a

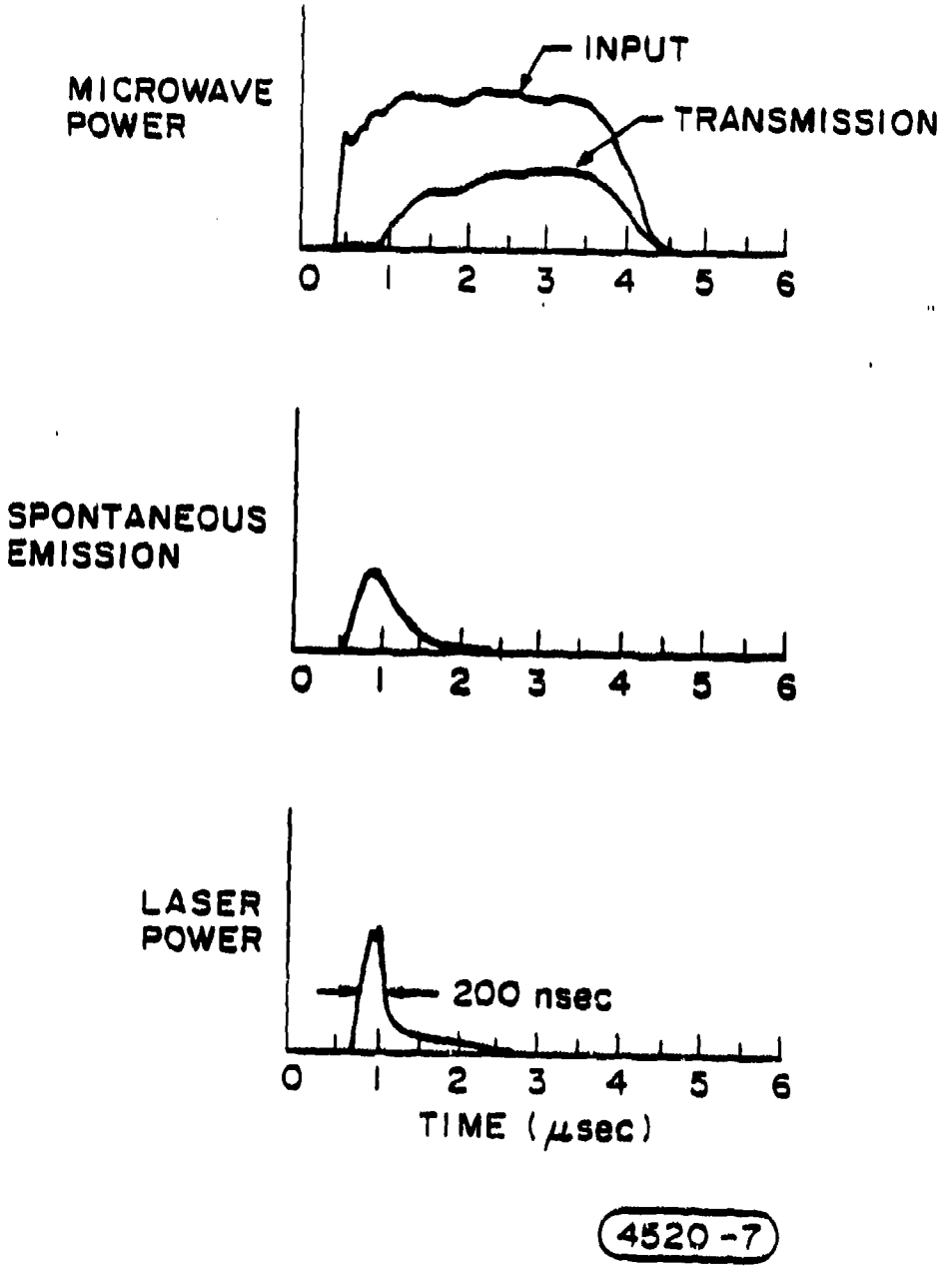

Fig. 5--High power behavior of microwave transmission, $XeCl^*$ spontaneous emission, and laser action.

1 mm wide bright ring was visible. However, the temporal development of this nonuniformity has not been studied and it seems likely that it develops late in the pulse and corresponds to the observed 50% decrease in absorption. Nevertheless, small skin depths and nonuniform electron density distribution across the plasma tube could ultimately limit the deposition of microwave power into high pressure gases.

A new cell design as shown in Fig. 6 has been constructed incorporating a ridged structure to locally increase the electric field in the vicinity of the plasma. The tube is recessed in the wall of the X-band guide so that the plasma is flush with the guide surface. This is to allow a larger ridge to be used in the cell and to reduce microwave reflection from the plasma column. The plasma tube is 20 cm long with a 1 mm i.d. bore compared to the 40 cm long, 3 mm i.d. tubes of previous designs. The smaller bore diameter was chosen to alleviate a plasma inhomogeneity as evidenced by the ~ 1 mm ring of visible fluorescence observed in the 3 mm i.d. tubes of previous geometries. The uniformity of the 1 mm plasma is currently being studied. The cavity is a 0.5 m confocal configuration giving a beam waist of 0.16 mm so that the fundamental transverse mode should nearly fill the bore.

The 1 mm bore diameter was chosen not only to provide some mode control and uniform excitation of the plasma but also to provide a smaller plasma volume. Direct coupling of the microwaves is used instead of the distributed coupling since the gas volume is 20 times smaller than in previous geometries. The smaller active volume in the ridged cell design has lowered the oscillation threshold from 100 kW of input microwave power to only 25 kW of input power. This translates into a significant improvement in cost since small 50 kW magnetrons are considerably more economical

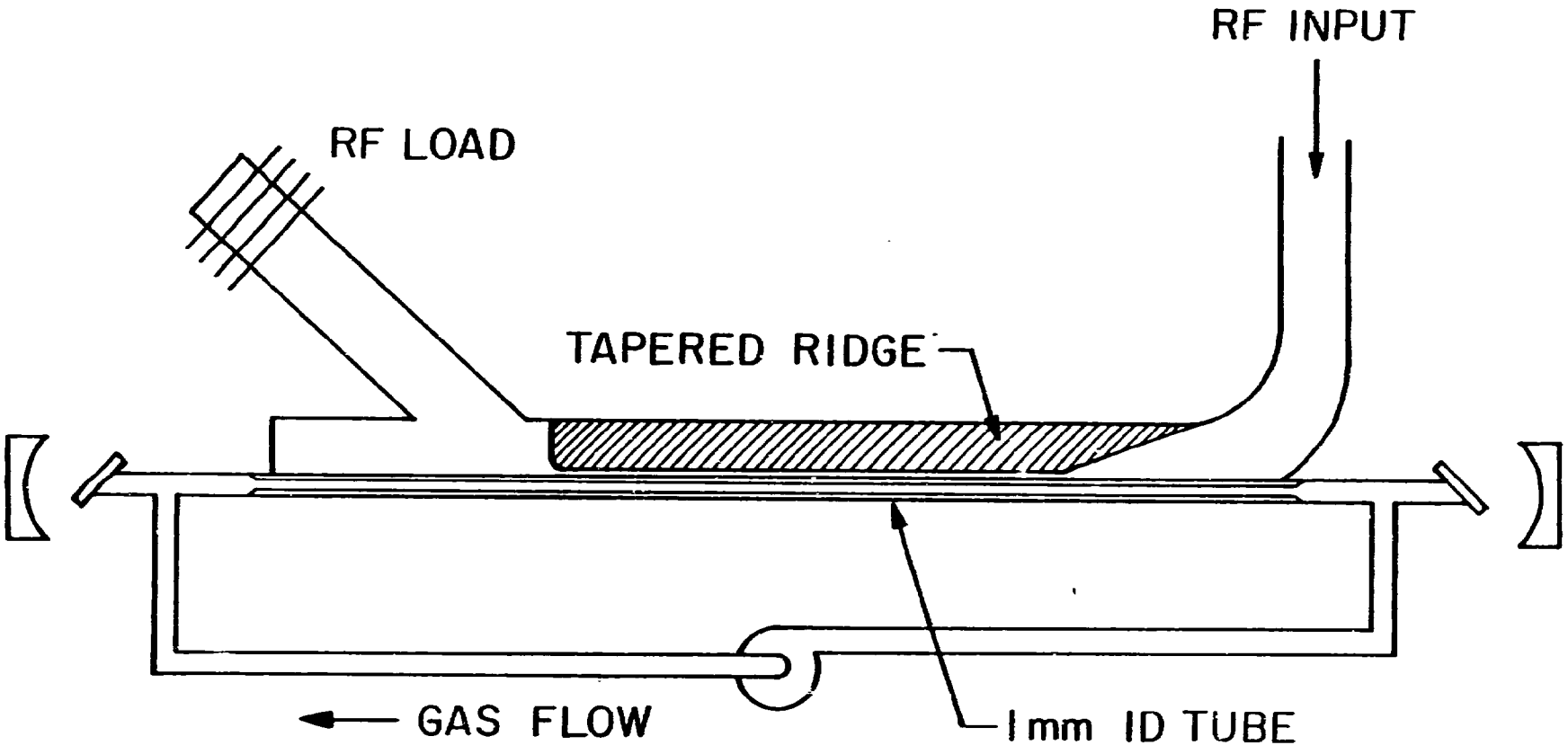

Fig. 6--Direct coupled cell with tapered ridge to increase E field in vicinity of plasma.

4520-10

than the 600 kW and 1.4 MW magnetrons used previously. The efficiency of the laser at low input powers has not yet been determined. Preionization appears to affect the laser oscillation threshold and output powers so that further improvements may result from including a spark gap in the recirculating system.

The laser pulse length in the ridged cell is 100 ns. Presently, a new cell is being constructed with an interchangeable section that will allow the length of the gain medium to be varied. This will determine whether the decrease in the laser pulse length to 100 ns from 200 ns is caused by the decrease in the length of the gain medium from 40 cm to 20 cm. If the laser is to be mode locked, however, the decrease in pulse length may not be significant since more roundtrips are available in a shorter cell.

The microwave pumping technique may have unique applications in the high pressure regime. This would be of considerable interest since laser oscillation in some excimer species such as Xe_2 and Xe_2Cl require pressures on the order of 10-20 atm. which are not easily attainable in conventional transverse electric discharges. We have shown efficient coupling of microwave energy into pure Ne at 17 atm. and laser oscillation in $XeCl^*$ at 10 atm. The dependence of the $XeCl^*$ output power at these high pressures is currently under study.

In general, future efforts will concentrate on optimizing laser pulse length for mode locking of the $XeCl^*$ laser. Further investigation into microwave pumping at high pressures may lead to improved efficiency for $XeCl^*$ and to applications in other excimers such as Xe_2 and Xe_2Cl.

C. ANTI-STOKES SPECTROSCOPY

1. Introduction

This program has supported the development of a new spectroscopic technique which allows the use of tunable laser technology for high resolution and picosecond time scale spectroscopy of core-excited atomic levels. This project has been jointly supported by NASA.

During this period the Office of Naval Research has supported a large effort aimed at the construction of a 200 Å laser. The work described here complements the ONR effort by focusing on the spectroscopy necessary for the laser development. In particular, we are interested in learning about core-excited levels whose autoionizing times are longer than their radiative times. In the alkali atoms, core-excited levels in the doublet series which have odd angular momentum and even parity, or even angular momentum and odd parity, are prohibited by LS selection rules from autoionizing into the ground ionic level. Also, if the valence electron is in a Rydberg state, autoionization times may be substantially increased.

Our work is based on spontaneous anti-Stokes scattering from atoms stored in a metastable level in an electrical discharge. The result is a radiation source which is tunable, narrow band, has prescribed polarization and, of special interest, may be of picosecond time scale. The maximum intensity of this radiation source is determined by the effective temperature of the storage level; for example, the $(1s2s)^1S$ level of He or Li^+. Since this level does not spontaneously decay, its accumulated population and, therefore, the peak source intensity, may exceed that of a radiating level by a factor of several thousand. To reach this peak intensity the applied visible laser must cause the media to become two-photon opaque to

the generated XUV radiation. In this sense the radiation source functions as a two-photon blackbody.

2. Development of the Anti-Stokes Spectroscopic Source

During this contract period, our work using the metastable helium level as a target state has resulted in a source which scans continuously from 535.4 → 558.4 Å, with a resolution of 3 mÅ. This continuous tunability was achieved by populating the metastable level more effectively using a pulsed microwave discharge. We have studied the inner shell absorption spectrum of potassium in this region, observing four narrow spectral features for the first time, and resolving lineshapes of previously identified absorption lines.

We have proposed extending this technique to other wavelength regions by utilizing storage states in other species; the other noble gasses and the alkali ions have spectra which may facilitate similar anti-Stokes light generation. Preliminary experiments to demonstrate the technique in neon are underway, and will be described.

In previous reports, the results obtained using a hollow-cathode He discharge were presented. That source operated with metastable populations of ~ 10^{11} atoms/cm^3, and generated low enough background XUV that no bandpass filtering (spectrometer) was required. The hollow cathode, however, required tunable laser pulses of 12 mJ or greater to achieve adequate signal-to-noise ratios. This is beyond the capabilities of commercially available dye lasers in some spectral regions. Therefore, we undertook development of a higher brightness, pulsed microwave-pumped source. The resulting source produces useable narrowband XUV with tunable dye laser inputs as low as 1 mJ. This improved source brightness is due primarily

to the higher metastable populations of ~ 10^{13} excited atoms/cm^3 achieved in the pulsed discharge.

In this source, 9.375 GHz microwave pulses are generated by a Varian SFD-303 magnetron driven by a line-type pulser. The 2 μs pulses had average powers of 500 kW, and are coupled into a quartz tube running the length of an 80 cm X-band waveguide as shown in Fig. 7. Dye laser pulses were injected into the quartz tube via a small right-angle prism and traveled the length of the tube. Backscattered radiation was collected by grazing reflections off the walls of the tube. The radiation passed through a hot potassium vapor absorption cell before entering the detection system. Along with the desired tunable radiation, the microwave heated He plasma emitted resonance-line radiation which was ~ 15 times more intense. To eliminate this overwhelming fixed-frequency noise source, a 1-meter vacuum monochrometer with slits wide open was used as a bandpass spectral filter. The transmitted anti-Stokes signal was then detected by an electron-multiplier tube. Despite the loss in signal due to the spectrometer, this system exhibits a S/N which is ~ 20 times better than the earlier hollow-cathode source.

We have used the apparatus with a Quanta-Ray PDL-1 pulsed dye laser over the 5960 - 7800 Å spectral region to generate 536.8 Å → 558.4 Å XUV. The 10 ns dye laser pulse can be triggered at variable delays after the start of the microwave pulse. The temporal behavior of the anti-Stokes emission, along with the resonance line background emission is shown in Fig. 8. As is apparent from the figure, the best ratio of anti-Stokes signal to background occurs late in the recombination tail. Unfortunately, operating in this regime, measured widths of potassium features were

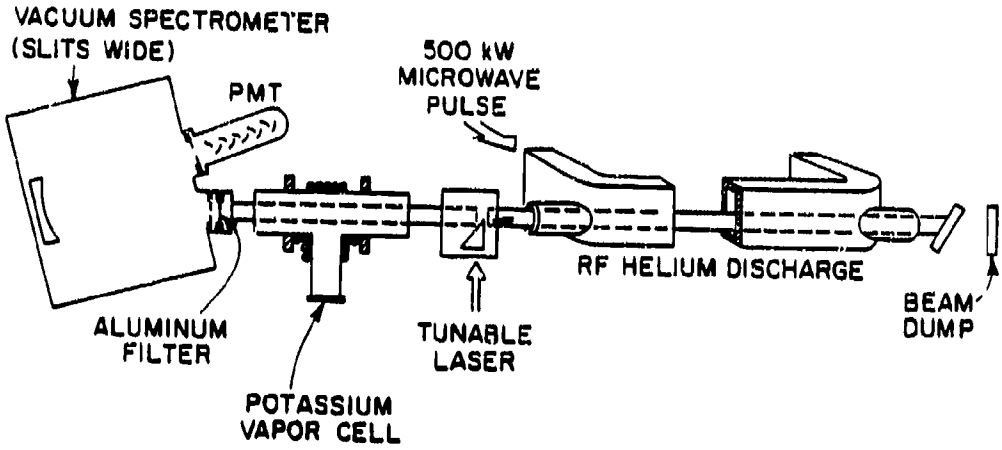

Fig. 7--Schematic of microwave pumped apparatus used for absorption spectroscopy of potassium.

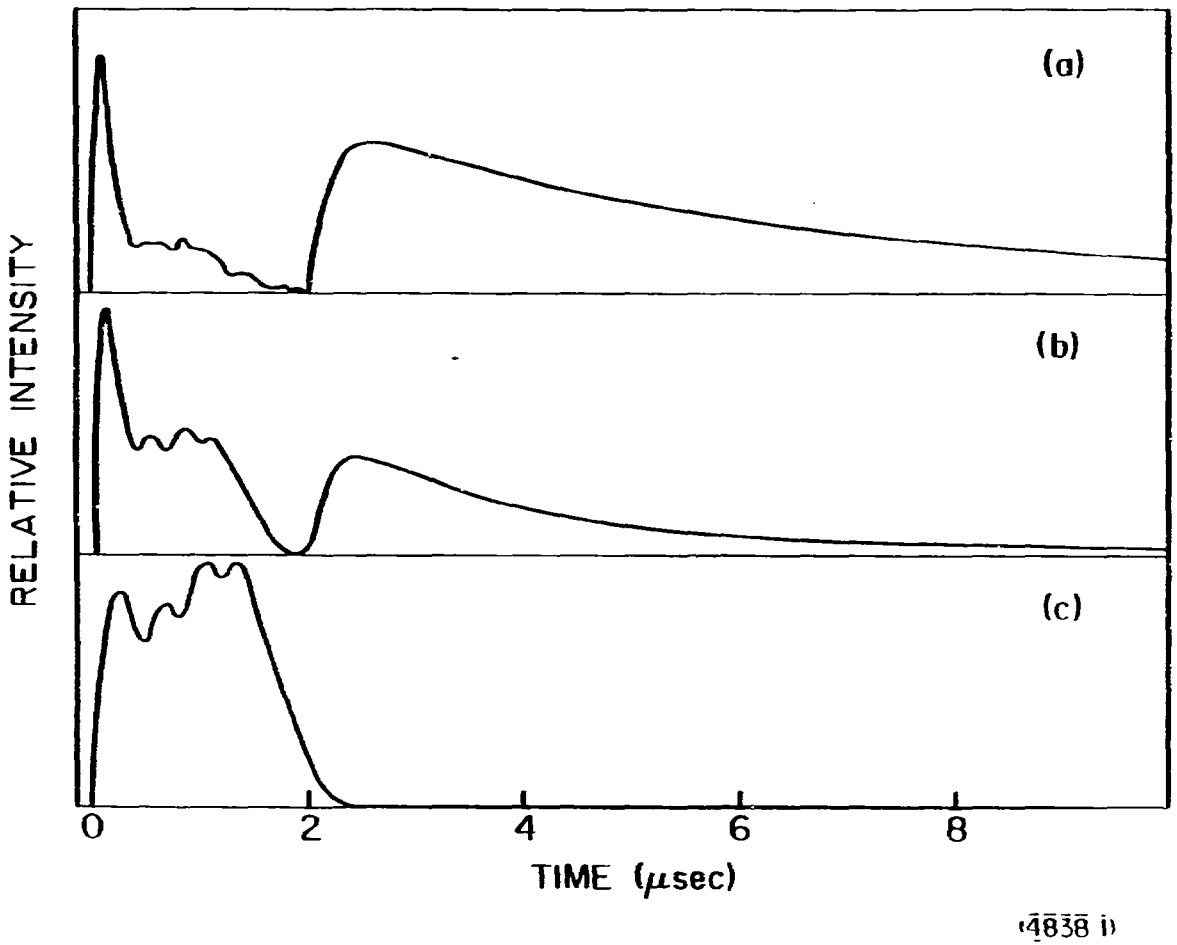

Fig. 8--Temporal behavior of microwave discharge emission.
(a) Anti-Stokes output at 550 Å.
(b) Resonance line emission at 584 Å.
(c) Input microwave pulse.

$\sim 2.5\ cm^{-1}$ wider than observed with the hollow-cathode apparatus. We attribute this to a heating of the helium during recombination, causing an increased Doppler width of the metastable level and thus the anti-Stokes radiation. We estimate the Doppler width as $3.5\ cm^{-1}$, corresponding to an atom kinetic temperature of $3000^{\circ}K$. To avoid this problem, we took spectra during the first few hundred nanoseconds after breakdown, during the avalanche period. In this mode, anti-Stokes linewidths were comparable to those observed using the hollow cathode, about $1.8\ cm^{-1}$.

A summary of features observed with these apparatuses are given in Tables 3 and 4. A sample spectra is shown in Fig. 9. It was obtained by scanning the dye laser in 0.18 Å steps (in the visible) under control of a microcomputer which was acquiring the data. Figure 9 is composed of 1024 points, scanned repetitively and summed to cancel long-term drifts.

Because this type of spectral source has tunability over only a small region near the energy of the metastable storage level, storage states in other species are being investigated in order to extend spectral coverage. We have considered using the other noble gasses and the corresponding isoelectronic alkali ions to access other spectral regions. An added complication of such species is that the preferred metastable storage state has the wrong parity for the anti-Stokes process. This is because p-electrons, rather than s-electrons, are being moved to create the metastable level. A solution is to resonantly transfer the population to a state of the same parity as ground with a low power fixed-frequency laser, and then to use an intense tunable pump to generate lower-sideband radiation. An example energy-level diagram for this scheme, using neon, is shown in Fig. 10. Figure 11 shows the potential spectral coverage of all the species mentioned.

Table 3

Potassium Absorption Features Observed with the

Hollow Cathode Apparatus

Energy	Linewidth	Designation	Previously Observed Energy
183320 ± 1 cm^{-1}	8.4 cm^{-1}	$3p^5 3d(^3P)5s\ ^2P_{1/2}$	183322 [a] cm^{-1}
183530	10.5	$3p^5 3d(^3P)5s\ ^2P_{3/2}$	183532 [a]
184008	2.6		
184076	3.4		184076 [b]
184321	2.5		
184344	15.0	$3p^5 4s(^1P)5s\ ^2P_{3/2}$	184342 [a]
184465	7.8	$3p^5 4d(^3P)5s\ ^2P_{1/2}$	184471 [a]
185806	1.9		
186659	5.0	$3p^5 4d(^1D)4s\ ^2D_{3/2}$	186656 [a]

[a] M. W. D. Mansfield (1975)

[b] G. Kavei, et al. (1977)

Table 4

Linewidths and Positions of Potassium Absorption Features

Observed with the Microwave Apparatus

Energy (cm^{-1})	Linewidth (cm^{-1})	Designation	Previously Observed Energy (cm^{-1})
179885	4.0	$3p^5 3d(^3D)4s\ ^2D^o_{3/2}$ [a]	179886 [a]
179918	2.1		179920
180547	43.0	$3p^5 3d(^1P)4s\ ^2P^o_{1/2}$	180551
180794	55.0 [b]	$3p^5 3d(^1P)4s\ ^2P^o_{3/2}$	180791
180840	11.0 [b]		180850
181519	2.7		181517
181745	5.5	$3p^5 3d5s\ ^4P^o_{3/2}$	181742
182152	8.8		182152
182652	5.6		182651

[a] Energies and designations from Mansfield

[b] Lines very asymmetric; linewidths determined from fit to theoretical Fano profile

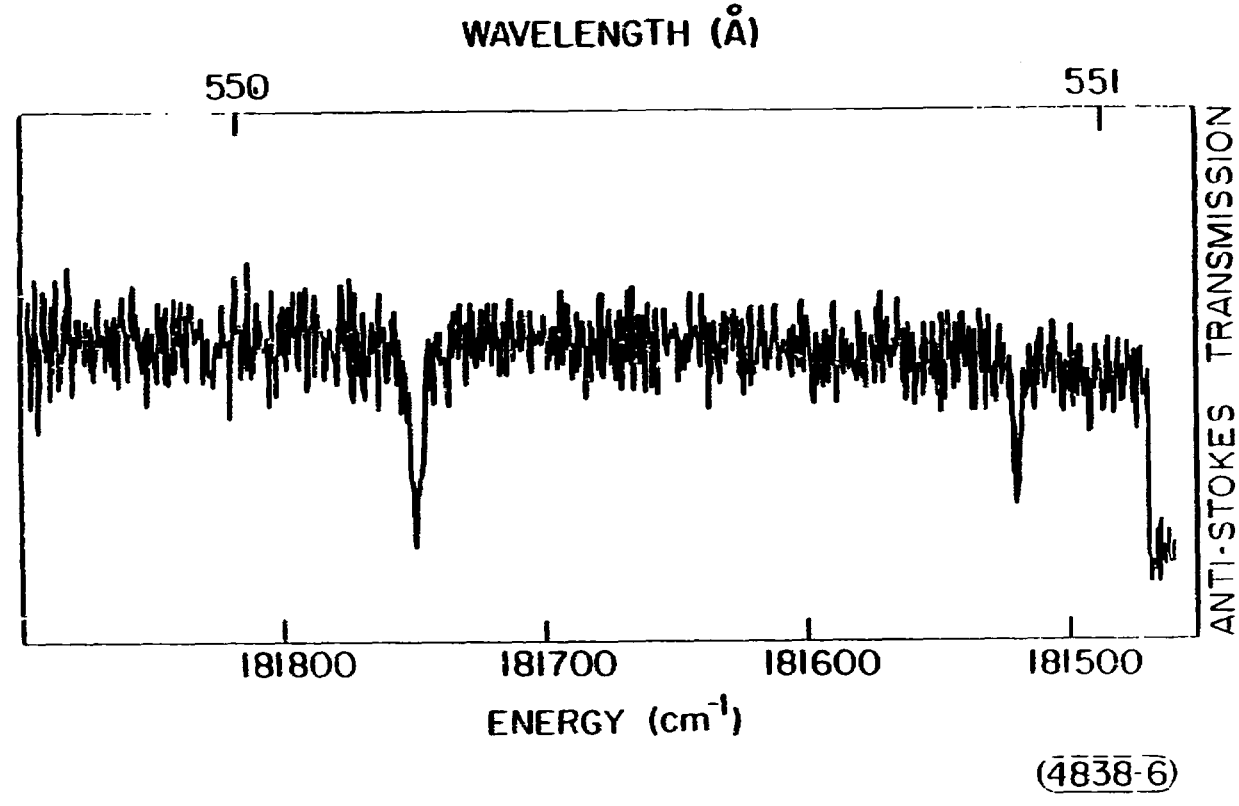

Fig. 9--Absorption scan of potassium obtained with microwave apparatus. Potassium cell length was 4.5 cm, density 1×10^{15} atoms/cm^3.

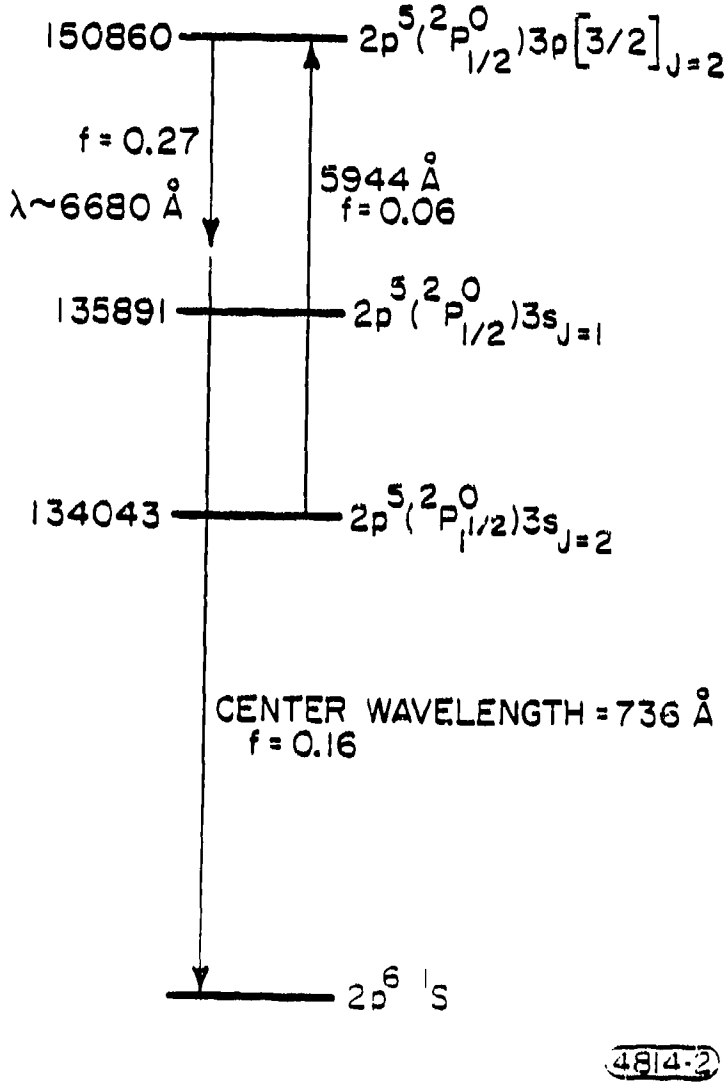

Fig. 10--Atomic energy level diagram showing levels relevant to Raman scattering in neon.

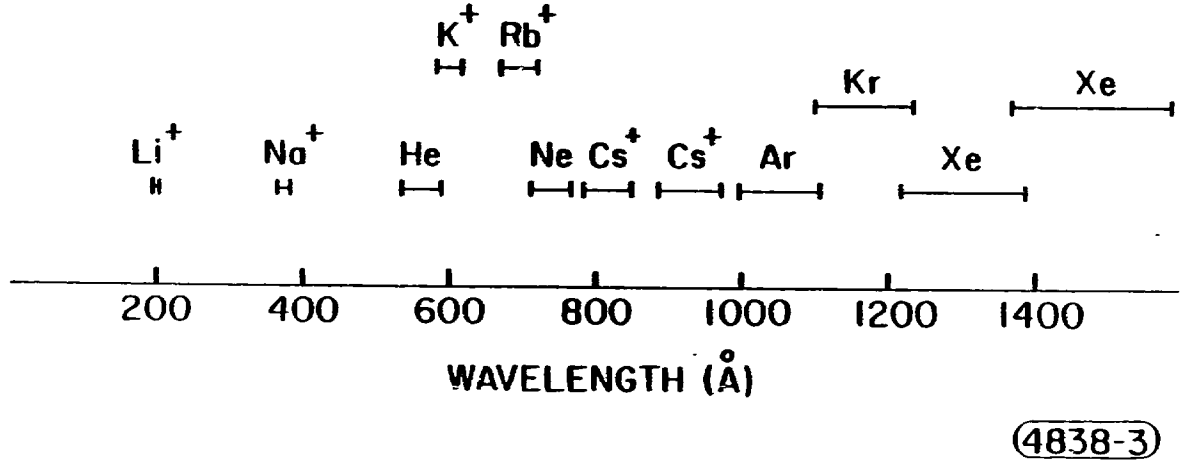

Fig. 11--Possible spectral regions which could be examined developing the spontaneous Raman source in various rare gasses and alkali ions.

We have begun investigating this system in neon as a prototype for this more-general two-laser source. With the same pulsed microwave apparatus as was used for the later work in helium, we have observed the resonant transfer of energy from (Fig. 11) the $2p^5[^2P^o_{3/2}]3s_{J=2}$ metastable state to the $[^2P^o_{1/2}]3p_{J=2}$ anti-Stokes upper state, using a dye laser tuned to 5944 Å. The transition was highly saturated with ~ 1 mJ, and subsequent fluorescence to the $[^2P^o_{1/2}]3s_{J=1}$ state was observed at 6678 Å. In fact, during the recombination period the 6678 transition became highly inverted and superfluorescence (lasing) without mirrors was observed. From the energy output at 6678 Å we can infer a lower bound on the population available at the upper level of the anti-Stokes process as $\sim 2 \times 10^{12}$ cm^{-3}. The present apparatus will require further modification to increase the optical transmission at 750 Å in order to observe the Raman process.

3. Two-Photon Spectroscopy of Li Using Anti-Stokes Radiation

The peak intensity of the tunable anti-Stokes emission relative to the background plasma emission, at constant laser pulse energy, varies inversely as the pulse length of the tunable laser pulse. However, to use this increased contrast, an XUV detector which is (effectively) as fast as the emission pulse is required.

One way of accomplishing this is to detect the emission (either electron or photon) from two-photon pumped autoionizing levels. In such an experiment one photon would come from a picosecond time scale anti-Stokes source while the other would be a visible photon of the energy required to access the selected level.

In the alkali atoms the levels prohibited from autoionizing by LS selection rules require access by two photons. For example, the non-autoionizing $(1s2p)^3P\ 3p\ ^2P$ level of Li can be accessed via the two-photon

route $1s^2 2s\ ^1S \rightarrow 1s^2 2p\ ^2P \rightarrow (1s2p)^3P\ 3p\ ^2P$. The first photon promotes the valence electron from a 2s to 2p orbit, while the second photon (the anti-Stokes photon) causes a $1s \rightarrow 3p$ core transition. Excitation of the $(1s2p)^3P\ 3p\ ^2P$ level can be detected by right angle observation of $1s2p(^3P)3p\ ^2P \rightarrow 1s2s(^3S)3p\ ^2P^o$ fluorescence at 5722 Å; or by observation of $1s2p(^3P)3p\ ^2P \rightarrow 1s2p\ ^2P^o$ XUV fluorescence at 197 Å.

During the past year, we have constructed an apparatus and performed preliminary experiments with the goal of using the anti-Stokes XUV flashlamp for two-photon absorption spectroscopy of core-excited states in neutral lithium. Two experiments are currently envisioned which will measure the position of the $(1s2p)^3P\ 3p\ ^2P$ and $(1s2p)^1P\ 3d\ ^2D$ core-excited states in Li I, both of which are of interest in the construction of a XUV laser. In the first (Fig. 12a), Li^+ metastable 1s2s ^1S states are created in a pulsed hollow-cathode discharge. Experiments by Falcone, et al. have shown that Li^+ metastable densities of up to 10^{12}/cc are obtainable in the hollow cathode. A laser at 9581 Å, the Li^+ 1s2s ^1S – 1s2p ^1P resonance, causes anti-Stokes emission at 501,808 cm^{-1}, ~ 199 Å. Applying a second laser at 5226 Å will cause absorption of the 199 Å radiation via the two-photon transition in Li I $1s^2 2s\ ^1S \rightarrow (1s2s)^3S\ 3p\ ^2P \rightarrow (1s2p)^3P\ 3p\ ^2P$. The detuning from the intermediate state is 1660 cm^{-1}. The cross section for the two-photon process is $\sigma(cm^2) = 1.1 \times 10^{-27} p(5226\ Å)/A\ (W/cm^2)$. Thus, for a 50 cm long Li cell at a density of 3×10^{16} Li/cm^3, power densities of ~ 5×10^8 W/cm^3 are needed for substantial absorption of the anti-Stokes light. With currently available lasers this is possible with beam sizes on the order of ~ 2 mm.

In the second experiment (Fig. 12b) a non-resonant 1.06 μm Nd:YAG laser is used to scatter off the Li^+ metastable ions and create anti-Stokes

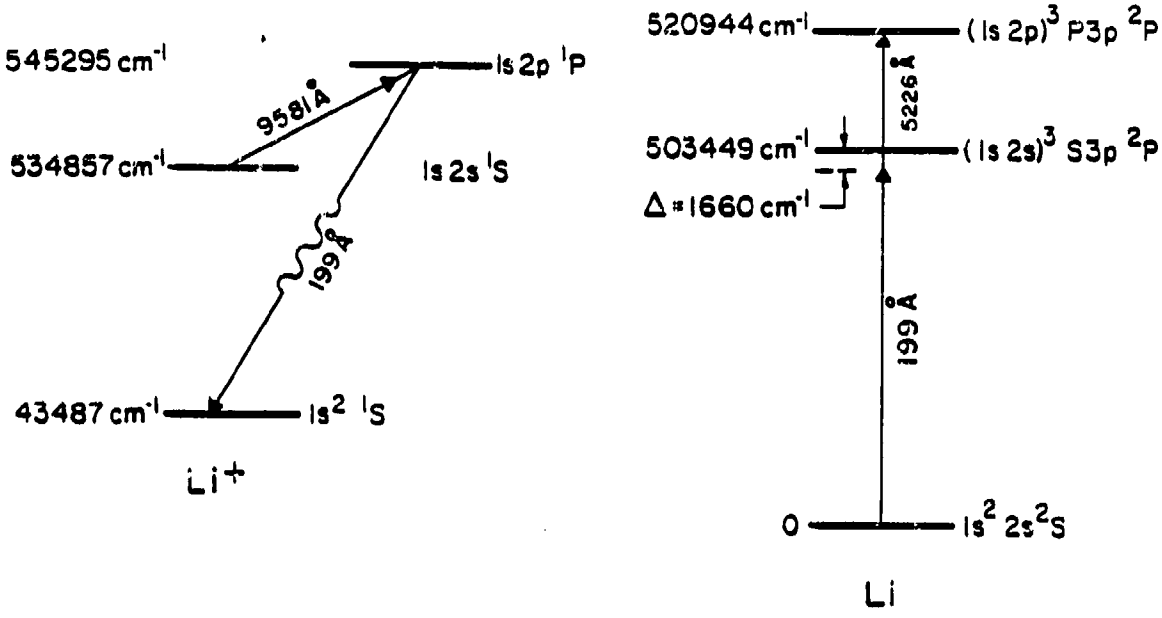

Fig. 12(a)--Two-photon absorption experiment using resonant Li^+ flashlamp.

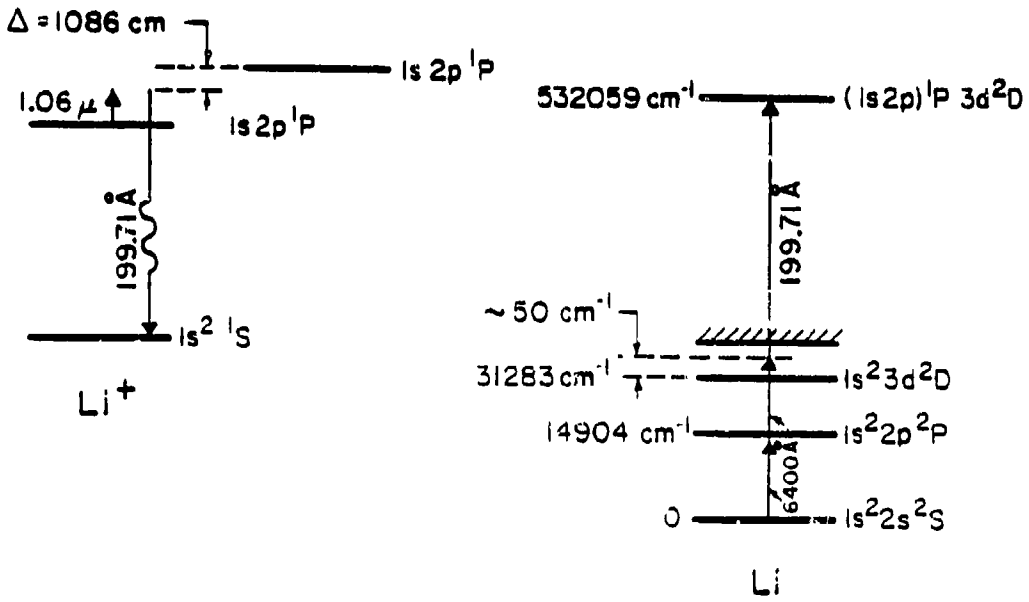

Fig. 12(b)--Two-photon absorption experiment using 1.06 μm pumped Li^+ flashlamp.

4908-1

light at 500,733 cm^{-1}. This wavelength is within 50 cm^{-1} of the $1s^2 3d\ ^2D$ – $(1s2p)^1P\ 3s\ ^2D$ transition in Li I. Two photons of a second applied laser at ~ 6400 Å make up the difference to ground and complete the two-photon transition. Because the detunings in the neutral are smaller than in the first experiment, larger absorptions are possible. The difficulty, however, is that the large flashlamp detuning (1086 cm^{-1}) requires a substantially larger laser than in the previous case to create sufficient anti-Stokes light.

The experimental set-up is shown in Fig. 13. A hollow-cathode discharge is followed by a 50 cm region of Li at a density of $\approx 3 \times 10^{16}$ which acts as an absorption cell. The cathode and detector are fitted with apertures which prevent any XUV radiation from entering the detector except that which has passed through the path defined by the laser (either 5226 Å or 6400 Å) which causes the two-photon absorption. The detector aperture is followed by a LiF slide which acts as a beamsplitter, transmitting the visible laser radiation out of the cell while reflecting the XUV component towards the detector. The XUV detector itself consists of a p-terphenyl scintillator and a fast photomultiplier tube. During the experiment, the laser is tuned while the XUV level is monitored for absorption.

At the present time, construction of the cell has been completed and we have succeeded in seeing the anti-Stokes radiation from the resonant (9581 Å) flashlamp. Currently we are attempting to optimize the level of this source by both increasing the collection efficiency of our detection system and experimenting with different modes of operation for the hollow-cathode discharge. This is necessary because the small beam sizes required

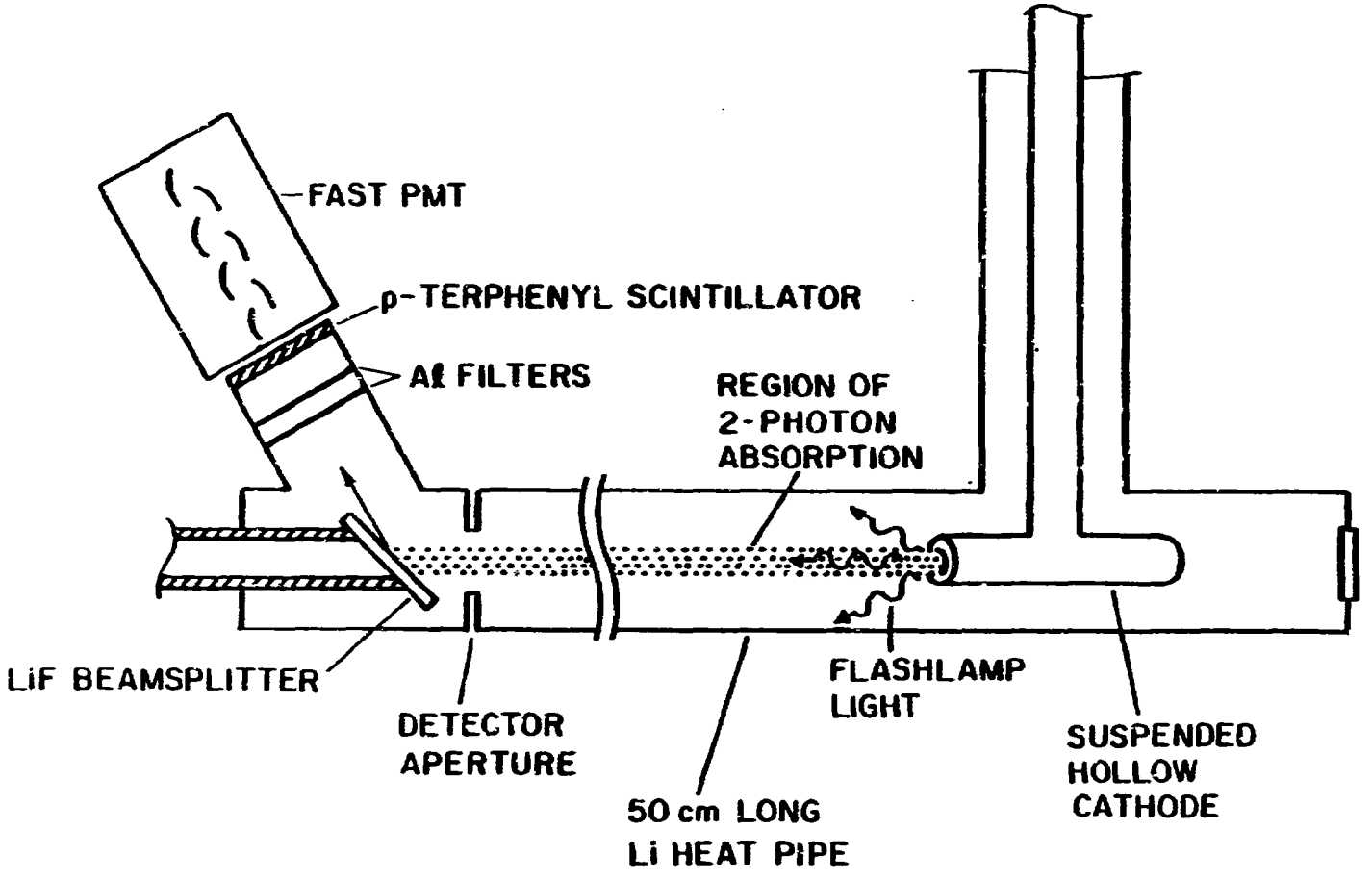

Fig. 13--Experimental design of two-photon absorption experiment.

4908-2

to obtain sufficient power density to create the two-photon absorption severely limit the solid angle for collection of the anti-Stokes radiation. We have also attempted to observe the anti-Stokes signal from the nonresonant 1.06 μm flashlamp but were unable to do so at the highest 1.06 μm power densities we were able to put through the cell. Progress in actually performing the absorption experiment has been somewhat limited by lack of a suitable combination of lasers to create both the flashlamp and the two-photon absorption. We are therefore examining an experiment in which the Li^+ $1s2p\,^1P - 1s^2\,^1S$ resonance line radiation will act as the light source rather than an anti-Stokes flashlamp. Although the detector has no wavelength discrimination, experiments in other discharges have shown that the 199 Å resonance radiation is by far the dominant component of the total XUV light from the discharge.

IV. PUBLICATIONS SUPPORTED

1. R. W. Falcone and G. A. Zdasiuk, "Pair Absorption Pumped Barium Laser," Optics Lett. 5, 155 (April 1980).
2. R. W. Falcone and G. A. Zdasiuk, "Radiative Collisional Fluorescence Observed From Thermally Excited Atoms," Optics Lett. 5, 365 (September 1980).
3. S. E. Harris, J. F. Young, R. W. Falcone, W. R. Green, D. B. Lidow, J. Lukasik, J. C. White, M. D. Wright, and G. A. Zdasiuk, "Laser Induced Collisional Energy Transfer," in Atomic Physics VII, D. Klepner and F. M. Pipkin, eds. (New York: Plenum Press, 1981).
4. A. J. Mendelsohn, R. Normandin, S. E. Harris, and J. F. Young, "A Microwave Pumped $XeCl^*$ Laser," Appl. Phys. Lett. 38, 603 (April 1981).
5. Joshua E. Rothenberg, J. F. Young, and S. E. Harris, "High Resolution XUV Spectroscopy of Potassium Using Anti-Stokes Radiation," Optics Lett. 6, 363 (August 1981).
6. M. D. Wright, D. M. O'Brien, J. F. Young, and S. E. Harris, "Laser Induced Charge Transfer Collisions of Calcium Ions With Strontium Atoms," Phys. Rev. A 24, 1750 (October 1981).
7. S. E. Harris, R. W. Falcone, M. Gross, R. Normandin, K. D. Pedrotti, J. E. Rothenberg, J. C. Wang, J. R. Willison, and J. F. Young, "Anti-Stokes Scattering as an XUV Radiation Source," in Laser Spectroscopy V, A. R. W. McKellar, T. Oka, and B. P. Stoicheff, eds. (New York: Springer-Verlag, 1981).

8. J. F. Young, S. E. Harris, P. J. K. Wisoff, and A. J. Mendelsohn, "Microwave Excitation of Excimer Lasers," Laser Focus (April 1982), p. 63.

9. S. E. Harris, J. F. Young, R. W. Falcone, Joshua E. Rothenberg, J. R. Willison, and J. C. Wang, "Anti-Stokes Scattering as an XUV Radiation Source and Flashlamp," in Laser Techniques for Extreme Ultraviolet Spectroscopy, R. R. Freeman and T. J. McIlrath, eds. (New York: AIP, 1982).

10. S. E. Harris, R. W. Falcone, and D. M. O'Brien, "Proposal for High Power Radiative Collisional Lasers," Optics Lett. 7, 397 (September 1982).

11. S. E. Harris, J. F. Young, R. W. Falcone, Joshua E. Rothenberg, and J. R. Willison, "Laser Techniques for Spectroscopy of Core-Excited Atomic Levels," in Proceedings of the CNRS International Colloquium on Atomic and Molecular Physics Near Ionization Thresholds in High Fields, Aussois, France, June 1982 (to be published).

12. P. J. K. Wisoff, A. J. Mendelsohn, S. E. Harris, and J. F. Young, "Improved Performance of the Microwave-Pumped XeCl Laser," IEEE J. Quant. Elect. QE-18, 1839 (November 1982).

V. LIST OF PERSONNELL

S. E. Harris

J. F. Young

R. W. Falcone

R. Normandin

A. J. Mendelsohn

P. J. K. Wisoff

D. P. Dimiduk

D. M. O'Brien

J. E. Rothenberg (Graduated October 1982)

M. D. Wright (graduated March 1981)

G. A. Zdasiuk (graduated December 1980)